



Supported palladium hydroxide-catalyzed intramolecular double C–H bond functionalization for synthesis of carbazoles and dibenzofurans

Tamao Ishida^{a,*}, Ryosuke Tsunoda^a, Zhenzhong Zhang^a, Akiyuki Hamasaki^a, Tetsuo Honma^b, Hironori Ohashi^c, Takushi Yokoyama^a, Makoto Tokunaga^{a,d,*}

^a Department of Chemistry, Graduate School of Sciences, Kyushu University, 6-10-1 Hakozaki, Higashi-ku, Fukuoka, 812-8581, Japan

^b Japan Synchrotron Radiation Research Institute (JASRI/SPring-8), 1-1-1 Kouto, Sayo, Hyogo, 679-5198, Japan

^c Faculty of Arts and Science, Kyushu University, 744 Motoooka, Nishi-ku, Fukuoka, 819-0395, Japan

^d International Research Center for Molecular Systems (IRCMS), Kyushu University, 744 Motoooka, Nishi-ku, Fukuoka, 819-0395, Japan

ARTICLE INFO

Article history:

Received 5 August 2013

Received in revised form

25 December 2013

Accepted 30 December 2013

Available online 8 January 2014

Keywords:

C–H functionalization

Carbazole

Dibenzofuran

Palladium hydroxide

Heterogeneous catalyst

ABSTRACT

Metal oxide-supported palladium hydroxide ($\text{Pd}(\text{OH})_2/\text{MO}_x$) catalysts enabled the oxidative intramolecular couplings of diarylamines to carbazoles and diarylethers to dibenzofurans via double aryl C–H bond functionalizations with molecular oxygen as the sole oxidant. While supported PdO, Pd, and palladium acetate catalysts showed poor catalytic activities, supported $\text{Pd}(\text{OH})_2$ exhibited remarkably high catalytic activity. Among supported $\text{Pd}(\text{OH})_2$ catalysts, $\text{Pd}(\text{OH})_2/\text{ZrO}_2$ was found to be an efficient catalyst in terms of catalytic activities and selectivities for the synthesis of carbazoles and dibenzofurans.

© 2014 Elsevier B.V. All rights reserved.

1. Introduction

Transition metal-catalyzed C–C bond formation reactions are particularly important reactions in fine chemical syntheses, and many reactions have been established by using organic halides and organometallic compounds such as Suzuki, Heck, and Negishi coupling reactions [1]. Although these methods can be utilized for versatile substrates under mild reaction conditions, large amounts of inorganic wastes are produced from these reactions. Over the past decades, to avoid the use of activated aryl halides, direct trans-formation of C–H bonds into C–C bonds has received significant attention [2].

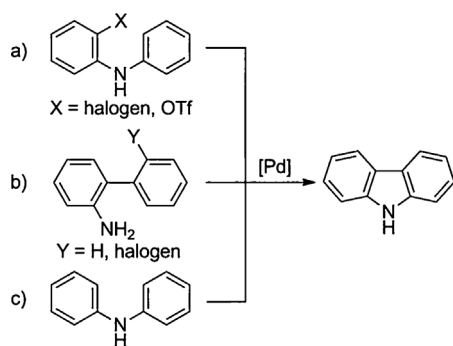
Carbazoles can be found in biologically active alkaloids [3] and are important compounds owing to photorefractive, photoconductive, hole-transporting, and light-emitting properties [4,5]. Although carbazole is produced by distillation of coal tar in industry, only small amounts can be obtained. To establish efficient processes for synthesizing carbazoles is of great interest, and several methods have been investigated in laboratories.

Representative synthetic protocols involving C–C or C–N bond formations are depicted in Scheme 1: (a) intramolecular coupling of C–X (X = halogen, triflate) and C–H bonds [6–10], (b) intramolecular C–N bond formation in [1,1'-biphenyl]-2-amine [11–14], and (c) intramolecular coupling of two C–H bonds of diphenylamine [15–20]. To avoid the use of aryl halides, Scheme 1b or c is more desirable. In C–H/N–H coupling (Scheme 1b), protecting groups are generally required at the nitrogen atom. Matsubara and co-workers reported the synthesis of carbazole from unprotected [1,1'-biphenyl]-2-amine over Pd/C [14]. However, high temperatures of over 250 °C are required. Since diphenylamine is readily available, the transformation of diphenylamine to carbazole (Scheme 1c) can be regarded as the most attractive route for carbazole synthesis. Moreover, water is a sole by-product when molecular oxygen can be utilized as an oxidant for the reaction.

The intramolecular oxidative coupling of two C–H bonds of diphenylamine to carbazole has been mainly studied using homogeneous palladium catalysts such as $\text{Pd}(\text{OAc})_2$ [15–20]. Although O_2 can be used as an oxidant, stoichiometric oxidant such as Ag_2O [18] or co-catalyst such as $\text{Cu}(\text{OAc})_2$ [20] have still been used. C–X/C–H coupling over heterogeneous catalysts has been reported using polymer-supported Pd nanoparticles (NPs) [21], $\text{Pd}(\text{OH})_2/\text{C}$ [22], and colloidal Pd NPs [23]. However, C–H/C–H bond coupling is limited [24,25]. Yin and co-workers reported

* Corresponding authors. Tel.: +81 92 642 7528; fax: +81 92 642 7528.

E-mail addresses: tishida@chem.kyushu-univ.jp (T. Ishida), mtok@chem.kyushu-univ.jp (M. Tokunaga).



Scheme 1. Synthetic methods of carbazole by C–H bond functionalization.

that heterogeneous carbon-supported Pd-polyoxometalate (POM) catalysts promoted the coupling of aryl C–H bond with sp^2 C–H bond of electron-deficient alkenes [24]. POM was responsible for high catalytic activity of Pd(II) species and worked as re-oxidation catalysts for Pd(0) species in the catalytic cycle. Direct aryl C–H/aryl C–H coupling over heterogeneous catalysts has been limited to the synthesis of 2,2'-bipyridines from pyridine derivatives [25].

In this work, we demonstrated that $\text{Pd}(\text{OH})_2/\text{ZrO}_2$ efficiently catalyzed the synthesis of carbazoles from diphenylamines using O_2 as the sole oxidant without the aid of re-oxidation catalysts. Dibenzofuran and its derivatives are also important chemicals, but examples are scarce compared to those for carbazole synthesis [15]. The intramolecular coupling of diphenylethers to obtain dibenzofurans was also studied using supported $\text{Pd}(\text{OH})_2$ catalysts.

2. Experimental

2.1. Materials

Palladium chloride (PdCl_2) was purchased from Tanaka Kikin-zoku KK. and used as received. Reagent grades $\text{Co}(\text{NO}_3)_2 \cdot 6\text{H}_2\text{O}$ was purchased from Kanto Kagaku Chemical. Carbon supported Pd catalysts, 10 wt% Pd/C and 20 wt% $\text{Pd}(\text{OH})_2/\text{C}$ were purchased from Sigma–Aldrich. All commercial starting materials and reagents were used as received. For the scope of substrate, 4-chlorodiphenylamine was synthesized according to the literature [26]. Al_2O_3 , TiO_2 (P-25), ZrO_2 (RC-100), and CeO_2 , were supplied by Wako Pure Chemical, Mizusawa Chemicals, Nippon Aerosil Co., Ltd., Daiichi Kigenso Kagaku Kogyo, and Shin-Etsu Chemical Co., Ltd., respectively.

2.2. Catalyst preparation

Metal oxide-supported $\text{Pd}(\text{OH})_2$ catalysts ($\text{Pd}(\text{OH})_2/\text{MO}_x$) were synthesized according to the literature [27] with minor modifications. Palladium chloride (PdCl_2) (177 mg) was dissolved in distilled water (1000 mL) containing 2 mL of conc. HCl. The pH of the solution was adjusted to 10 by adding 1.0 M NaOH aqueous solution. The metal oxide support (1.0 g) was added to the solution at 70 °C. The pH of the solution was adjusted to 10 by adding 1.0 M NaOH aqueous solution, if necessary. The suspension was cooled to room temperature and stirred at room temperature for 24 h. The solid was filtered, washed with water, and then dried in air at 100 °C for 12 h.

For the preparation of 20 wt% $\text{Pd}(\text{OH})_2/\text{ZrO}_2$, PdCl_2 (417 mg) was dissolved in an aqueous solution of conc. HCl (10 mL) and distilled water (240 mL). The solution was warmed to 60 °C and the pH of the solution was adjusted to 8.0 by adding 0.1 M NaOH aqueous solution. Then, the support (1.0 g) was added to the

solution and the suspension was stirred at 70 °C for 1 h. The solid was filtered, washed with water, and then dried in air at 70 °C overnight.

10 wt% PdO/ZrO_2 was prepared by impregnation followed by calcination in air at 300 °C for 4 h. 20 wt% Pd/ZrO₂ and 20 wt% PdO/ZrO_2 catalysts were prepared from 20 wt% $\text{Pd}(\text{OH})_2/\text{ZrO}_2$ treated in a flow of H_2 at 300 °C for 4 h and calcination in air at 300 °C for 4 h, respectively.

2.3. Characterization

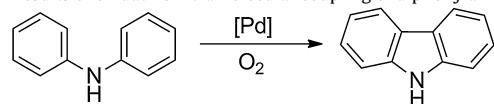
High angle annular dark-field scanning transmission electron microscopy (HAADF-STEM) observations were performed using JEOL JEM-ARM200F operating at 200 kV at the research laboratory for high vacuum electron microscopy (HVEM), Kyushu University. Palladium contents in the catalysts and leaching of palladium into the reaction solutions were analyzed by microwave plasma-atomic emission spectrometry (MP-AES) by Agilent, 4100 MP-AES. The reaction solution was filtered to remove solid catalysts and the concentration of Pd in filtrate was analyzed by MP-AES. Fourier transform infrared (FT-IR) spectra of catalysts were obtained by JASCO FT-IR 6100 with an attenuated total reflection (ATR) accessory equipped with a single reflection ZnSe.

X-ray absorption fine structure (XAFS) measurements were performed at BL14B2 beamline of SPring-8 (Hyogo, Japan) [28,29]. The XAFS samples were ground with boron nitride in an agate mortar and were compacted into pellets. Pd K-edge (24.3 keV) XAFS spectra were measured using a Si(311) double crystal monochromator in transmission mode. Ionization chambers were used, and the quick scan technique (QXAFS) was used in these measurements. The spectral analysis was performed using the XAFS analysis software, Athena [30]. The extraction of the extended X-ray absorption fine structure (EXAFS) oscillation from the spectra, normalization by edge-jump, and Fourier transformation were performed using the Athena software.

Conversions and product yields were analyzed by gas chromatography (GC) using Agilent GC 6850 Series II equipped with FID and a J&W HP-1 column (0.25 μm thickness, 0.25 mm I.D., 30 m) using tridecane as an internal standard. ^1H and ^{13}C NMR spectra were recorded on a JEOL JNM-ECS400 spectrometer at 400 and 100 MHz, respectively and were shown in Supplementary data. ^1H assignment abbreviations are the following; singlet (s), doublet (d), triplet (t), and multiplet (m). Analytical thin-layer chromatography (TLC) was performed with Merck, TLC silica gel 60 F_{254} plates. Column chromatography was performed on silica gel (Kanto Chemicals, Silica gel 60 N, spherical, neutral, particle size 40–100 μm). Recycling preparative HPLC was performed on Japan Analytical Industry Co., Ltd., LC-908. Elemental analyses were carried out at the center of elementary analysis, Kyushu University.

2.4. General procedure for intramolecular oxidative coupling

To an autoclave was charged with diphenylamine (1 mmol), 10 wt% $\text{Pd}(\text{OH})_2$ catalyst (50 mg, Pd 5 mol%), solvent (3.0 mL), and a magnetic stirring bar. The autoclave was purged and filled with O_2 until the pressure reached 0.25 MPa. The reaction mixture was stirred at 100 °C for 12 h. After the reaction, the mixture was filtered, and the filtrate was analyzed by GC using tridecane as an internal standard. Intramolecular oxidative couplings of diarylamines and diarylethers were also performed in a similar manner. Characterization and NMR charts of the isolated compounds were listed in the supplementary data.

Table 1
Results of oxidative intramolecular coupling of diphenylamine over Pd(OH)₂/C.^a

Entry	Catalyst	Pd (mol%)	Solvent ^b	O ₂ (MPa)	Conv. (%) ^c	Yield (%) ^c
1	Pd(OH) ₂ /C	10	AcOH	0.5	98	24
2	Pd(OH) ₂ /C	10	AcOH–TFA (1/1)	0.5	95	30
3	Pd(OH) ₂ /C	10	AcOH–toluene (1/1)	0.5	94	33
4	Pd(OH) ₂ /C	10	AcOH–THF (1/1)	0.5	95	30
5	Pd(OH) ₂ /C	10	AcOH–CHCl ₃ (1/1)	0.5	46	24
6	Pd(OH) ₂ /C	10	AcOH–H ₂ O (1/1)	0.5	93	13
7	Pd(OH) ₂ /C	10	AcOH–dioxane (1/1)	0.5	87	61
8	Pd(OH) ₂ /C	10	1,4–Dioxane	0.5	8	1
9 ^d	Pd(OH) ₂ /C	10	AcOH–dioxane (1/1)	0.5	92	40
10	Pd(OH) ₂ /C	10	AcOH–dioxane (1/1)	0.25	82	60
11	Pd(OH) ₂ /C	10	AcOH–dioxane (1/1)	0.1	49	45

^a Reaction conditions: diphenylamine (1 mmol), catalyst, solvent (3 mL), O₂, 100 °C, 12 h.^b Parentheses indicate volumetric ratio.^c Calculated on the basis of GC analysis using tridecane as an internal standard.^d Hydroquinone (0.1 mmol).

2.5. Recycling test

After the reaction, the catalyst was recovered by filtration, washed with CH₂Cl₂ and MeOH, and dried in air at 100 °C for 12 h. The catalyst was used for the next run.

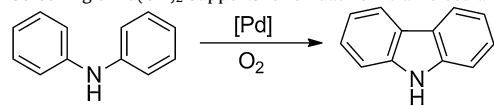
3. Results and discussion

3.1. Optimization of reaction conditions

Initially, we explored the oxidative intramolecular coupling of diphenylamine over commercially available Pd(OH)₂/C (Pearlman's catalyst) (Table 1). Generally, Pd-catalyzed oxidative couplings proceeds efficiently with carboxylic acids as solvents or additives, and acetic acid (AcOH) is frequently used [31–36]. Pd(OH)₂/C allowed the reaction to proceed to give carbazole in 24% yield (entry 1). Trifluoroacetic acid (TFA) is also reported to have beneficial effect [31–33], but the mixture of TFA and AcOH was not effective (entry 2). The synthesis of carbazole in mixed solvents, including AcOH, was also tested. The use of toluene and THF as co-solvents slightly

improved carbazole yields (entries 3 and 4). However, CHCl₃ and water were not effective (entries 5 and 6). In contrast, the mixture of AcOH and 1,4-dioxane remarkably improved the yields of carbazole (entry 7), whereas the reaction did not proceed in 1,4-dioxane (entry 8). Although the addition of hydroquinone as a radical scavenger caused a slight decrease in yield, carbazole was still obtained in 40% yield (entry 9). Thus, it can be assumed that peroxy radicals, which can be formed by the decomposition of 1,4-dioxane, does not play a major role as the oxidant in this transformation. A decrease in O₂ pressure from 0.5 MPa to 0.25 MPa did not affect carbazole yield (entry 10), but a further decrease in the O₂ pressure lowered yield in spite of better material balance (entry 11).

Further, support materials for Pd(OH)₂ were screened (Table 2). Metal oxide-supported Pd(OH)₂ catalysts (entries 1–5) showed similar or superior catalytic activities to those of Pd(OH)₂/C (Table 1, entry 10) except for Pd(OH)₂/Co₃O₄ (entry 3). Low catalytic activities for Pd(OH)₂/Co₃O₄ was due to dissolution of Co₃O₄ into AcOH during reactions. Amphoteric metal oxides (Al₂O₃ and ZrO₂) were appeared to be better supports than relatively acidic (TiO₂), basic (CeO₂), and inert (C) supports. It has been reported that acid-base properties of supports can control the oxidation state

Table 2
Screening of Pd(OH)₂ supports for oxidative intramolecular coupling of diphenylamine.^a

Entry	Catalyst	Pd (mol%)	Solvent ^b	Conv. (%) ^c	Yield (%) ^c
1	Pd(OH) ₂ /Al ₂ O ₃	5	AcOH–dioxane (1/1)	97	78
2	Pd(OH) ₂ /TiO ₂	5	AcOH–dioxane (1/1)	99	59
3	Pd(OH) ₂ /Co ₃ O ₄	5	AcOH–dioxane (1/1)	51	31
4	Pd(OH) ₂ /ZrO ₂	5	AcOH–dioxane (1/1)	99	85
5	Pd(OH) ₂ /CeO ₂	5	AcOH–dioxane (1/1)	68	41
6	Pd(OH) ₂ /ZrO ₂	0.5	AcOH–dioxane (1/1)	45	35
7	Pd(OH) ₂ /ZrO ₂	10	PrCO ₂ H–dioxane (1/1)	81	59
8	Pd(OH) ₂ /ZrO ₂	10	PivOH–dioxane (1/1)	61	54
9	Pd(OH) ₂ /ZrO ₂	10	TFA–dioxane (1/1)	28	0
10	Pd(OH) ₂ /ZrO ₂	10	HCO ₂ H–dioxane (1/1)	10	0
11	Pd(OAc) ₂ /ZrO ₂	5	AcOH–dioxane (1/1)	54	9
12	PdCl ₂	5	AcOH–dioxane (1/1)	56	24
13	Pd(OAc) ₂	5	AcOH–dioxane (1/1)	19	7
14	Pd(OH) ₂	5	AcOH–dioxane (1/1)	5	4

^a Reaction conditions: diphenylamine (1 mmol), catalyst, solvent (3 mL), O₂ (0.25 MPa), 100 °C, 12 h.^b Parentheses indicate volumetric ratio.^c Calculated on the basis of GC analysis using tridecane as an internal standard.

of supported Pd NPs [37,38]. Thus, acid-base properties of ZrO_2 may affect to stabilize Pd(II) state during reactions (entry 4). The reaction also proceeded in the presence of 0.5 mol% Pd (entry 6). The solvent effect of carboxylic acid was examined. The mixture of butanoic acid (PrCO_2H) or pivalic acid (PivOH) with 1,4-dioxane showed positive effect on the carbazole yield as AcOH –dioxane mixture did (entries 7 and 8), whereas TFA and formic acid gave poor results (entries 9 and 10). Homogeneous Pd catalysts (PdCl_2 , $\text{Pd}(\text{OAc})_2$, $\text{Pd}(\text{OH})_2$) showed much lower catalytic activities than supported $\text{Pd}(\text{OH})_2$ catalysts did, probably due to the formation of Pd black during the reaction (entries 12–14). Interestingly, the catalytic activity of $\text{Pd}(\text{OAc})_2/\text{ZrO}_2$, prepared by impregnation, was inferior to that of $\text{Pd}(\text{OH})_2/\text{ZrO}_2$ (entry 11). Amounts of leached Pd into the reaction solution after the reaction were estimated by MP-AES. The leached Pd was slightly lower for $\text{Pd}(\text{OH})_2/\text{ZrO}_2$ (10%) than that for $\text{Pd}(\text{OAc})_2/\text{ZrO}_2$ (13%). It indicated that $\text{Pd}(\text{OAc})_2$ was prone to dissolve in AcOH and leached Pd would aggregate to form Pd black, decreasing the catalytic performance.

3.2. Synthesis of dibenzofuran

Synthesis of dibenzofuran from diphenylether was also examined with several kinds of supported $\text{Pd}(\text{OH})_2$ catalysts (Table 3). Since diphenylether is less reactive, compared to diphenylamine, harsh reaction conditions with longer reaction times are generally required. As with the synthesis of carbazole, $\text{Pd}(\text{OH})_2/\text{ZrO}_2$ exhibited the highest catalytic activity and selectivity for dibenzofuran synthesis (entry 3). Although dibenzofuran was obtained in low yield in AcOH (entry 11), the use of PivOH remarkably improved the yield of dibenzofuran (entry 8), as mentioned by Fagnou and co-workers that the use of PivOH was effective to prevent side reactions such as dimerization and decomposition of the substrate via acyloxylation, thereby giving higher yield of desired coupling compounds than that in AcOH [15]. Higher reaction temperatures (entry 5) and concentrations (entry 9) improved the dibenzofuran yields. PdO/ZrO_2 (entry 6) and Pd/ZrO_2 (entry 7) also catalyzed the oxidative coupling of diphenylether, although the catalytic activities were inferior to $\text{Pd}(\text{OH})_2/\text{ZrO}_2$. Surface of Pd on ZrO_2 would be readily oxidized under the pressurized O_2 to form catalytically active Pd(II) species. Consequently, dibenzofuran was obtained in 80% yield under the optimized conditions in the presence of $\text{Pd}(\text{OH})_2/\text{ZrO}_2$ (entry 9).

3.3. Scope of substrates

The scope of substrates was investigated, and the results are shown in Table 4. The reactions of electron-rich diarylamines are known to be challenging [17]. Reactions of diarylamines with electron-donating groups proceeded smoothly by lowering the temperature to afford the corresponding carbazoles in good yields (entries 1–5). The reactivity in the oxidative coupling was influenced by the substitution pattern of diarylamines.[16] Specifically, 3-methoxydiphenylamine was more reactive than 4-methoxydiphenylamine and was converted to the corresponding carbazole in better yield (entries 1 and 2). This was ascribed to the fact that electron-donating groups at the *m*-position of diphenylamine would increase electron density at the *o,p*-positions, thereby accelerating the attack by electron-deficient Pd(II) species. The reaction of *o*-methylated diarylamine was inhibited presumably due to the inhibition of the coordination of the nitrogen atom to Pd(II) species by steric hindrance (entry 6). Diarylamines with electron-withdrawing groups were less reactive and the corresponding carbazoles were obtained in low to moderate yields (entries 7–10). The oxidative coupling of diarylethers also proceeded to give dibenzofurans and the reaction tendency was similar to that of diarylamines (entries 11–18).

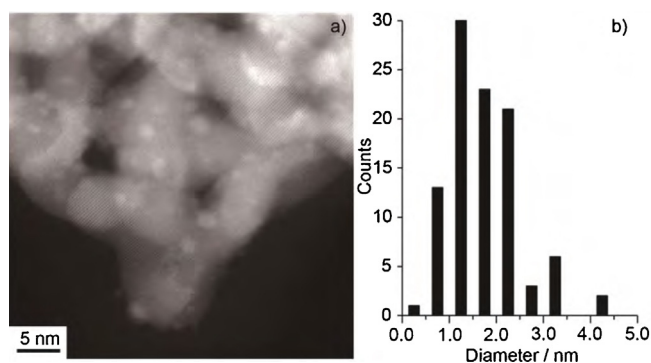


Fig. 1. HAADF-STEM image (a) and the size distribution of $\text{Pd}(\text{OH})_2$ nanoparticles (b) of 10 wt% $\text{Pd}(\text{OH})_2/\text{ZrO}_2$.

4-Chlorodiphenylamine and 4-chlorodiphenylether were also converted into the 3-chlorocarbazole and 2-chlorodibenzofuran in moderate yields, respectively (entries 7, 13, and 14), while the reaction of brominated substrates resulted in low yields (entries 8 and 15). As for 4-bromodiphenylamine, the reaction showed a good material balance, and certain amount of debrominated diphenylamine and carbazole were not formed (entry 8). However, for 4-bromodiphenylether, 7% yield of debrominated diphenylether was formed (entry 15). It suggested that oxidative addition of 4-bromodiphenylether to Pd(0), which was formed in-situ, occurred to produce debrominated substrate, diphenylether. We conducted the oxidative coupling of diphenylether in the presence of equimolar amount of bromobenzene. As a result, 14% of bromobenzene was converted and benzene was detected. At the same time, the oxidative coupling of diphenylether was significantly inhibited. It is likely that Pd is deactivated once Pd–Br bond is formed, although Pd–Cl bond does not affect the catalyst activity.

3.4. Characterization of catalysts

In order to evaluate the size of Pd NPs, HAADF-STEM observations were performed. $\text{Pd}(\text{OH})_2$ NPs of the fresh 10 wt% $\text{Pd}(\text{OH})_2/\text{ZrO}_2$ were highly dispersed on ZrO_2 , and the mean diameter of $\text{Pd}(\text{OH})_2$ NPs was calculated to be 1.8 ± 0.9 nm (Fig. 1). PdO was deposited on ZrO_2 as NPs in the range of 2–3 nm (supplementary data). The size of $\text{Pd}(\text{OH})_2$ NPs on ZrO_2 slightly increased with the mean diameter of 2.5 ± 0.9 nm after the first run for the synthesis of carbazole, but significant aggregation of $\text{Pd}(\text{OH})_2$ NPs was not observed.

Fig. 2 shows Pd K-edge XANES spectra of Pd foil, PdO, and $\text{Pd}(\text{OH})_2/\text{ZrO}_2$ including reference Pd foil, PdO, and $\text{Pd}(\text{OH})_2$. The spectra of PdO/ZrO_2 and $\text{Pd}(\text{OH})_2/\text{ZrO}_2$ resembled both PdO and

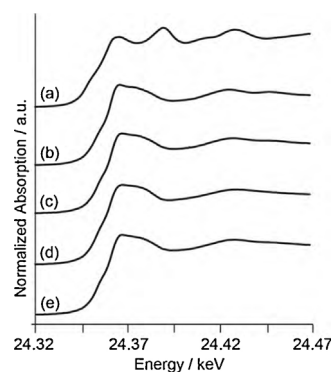
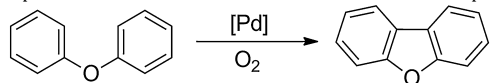


Fig. 2. Pd K-edge XANES spectra of Pd foil (a), PdO (b), 10 wt% PdO/ZrO_2 (c), $\text{Pd}(\text{OH})_2$ (d), 10 wt% $\text{Pd}(\text{OH})_2/\text{ZrO}_2$ (e).

Table 3
Optimization of reaction conditions for the oxidative coupling of diphenylether.^a

Entry	Catalyst	PivOH (g)	Temp. (°C)	Time (h)	Conv. (%) ^b	Yield (%) ^b
1	Pd(OH) ₂ /Al ₂ O ₃	2.0	120	60	55	49
2	Pd(OH) ₂ /TiO ₂	2.0	120	60	53	49
3	Pd(OH) ₂ /ZrO ₂	2.0	120	64	61	54
4	Pd(OH) ₂ /CeO ₂	2.0	120	48	44	41
5	Pd(OH) ₂ /ZrO ₂	2.0	130	48	65	62
6	PdO/ZrO ₂	2.0	130	48	59	42
7	Pd/ZrO ₂	2.0	130	48	38	35
8 ^c	Pd(OH) ₂ /ZrO ₂	2.0	130	48	64	58
9 ^c	Pd(OH) ₂ /ZrO ₂	0.7	130	48	88	80
10 ^d	Pd(OH) ₂ /ZrO ₂	0.7	130	48	80	69
11 ^{d,e}	Pd(OH) ₂ /ZrO ₂	–	130	48	100	26

^a Reaction conditions: diphenylether (1 mmol), 30 wt% Pd catalyst (50 mg, Pd 14 mol%), PivOH, O₂ (0.5 MPa).^b Calculated on the basis of GC analysis using tridecane as an internal standard.^c 20 wt% Pd(OH)₂/ZrO₂ (30 mg, Pd 6 mol%).^d 10 wt% Pd(OH)₂/ZrO₂ (30 mg, Pd 3 mol%).^e AcOH (3 mL).

Pd(OH)₂, assuming that the chemical state of Pd was Pd(II). However, PdO or Pd(OH)₂ could not be distinguished by XANES spectra due to the fact that spectral features of PdO and Pd(OH)₂ were almost identical. In the *k*³-weighted EXAFS oscillations, the amplitude of Pd(OH)₂ was lower than that of PdO in the range of 7–11 Å^{−1} (Fig. 3). The amplitude of PdO/ZrO₂ was slightly lower than that of reference PdO. The amplitude of Pd(OH)₂/ZrO₂ further decreased and became close to that of reference Pd(OH)₂. In the radial struc-

ture functions (RSF), two peaks were observed at 1.5 and 2.9 Å (phase-uncorrected) in PdO, and these peaks corresponded to Pd–O bond of the first coordination shell and both of Pd–Pd and Pd–O bond of the second one, respectively [38–41] (Fig. 4). In PdO/ZrO₂, FT magnitude of the peak at 2.9 Å decreased as compared to reference PdO. Decrease in FT magnitude of the second coordination shells for PdO/ZrO₂ can be produced by a disorder in the crystal structure of PdO and/or a small size of PdO NPs. In the RSF of Pd(OH)₂/ZrO₂, FT magnitude was lower than that of PdO/ZrO₂, but was higher than that of reference Pd(OH)₂. This result suggested that possibilities of (i) the presence of Pd(OH)₂ with PdO NPs, and/or (ii) the presence of smaller PdO NPs than PdO/ZrO₂, although the formation of Pd(OH)₂ cannot be fully asserted by XAFS.

XAFS measurements of Pd(OH)₂/ZrO₂ after the synthesis of carbazole was also carried out. After the reaction, the near-edge peak of XANES spectra at 24.37 keV decreased (Fig. 5a). *k*³-Weighted EXAFS oscillation pattern changed from the fresh catalyst and slightly resembled that of Pd foil (Fig. 5b). Moreover, FT magnitude of the peak at 1.5 and 2.9 Å in the RSF decreased (Fig. 5c). Instead, a new peak was observed at 2.5 Å, which corresponds to Pd–Pd bonds as seen in Pd foil. These results suggested that Pd(0) NPs also contained in Pd(OH)₂/ZrO₂ after use.

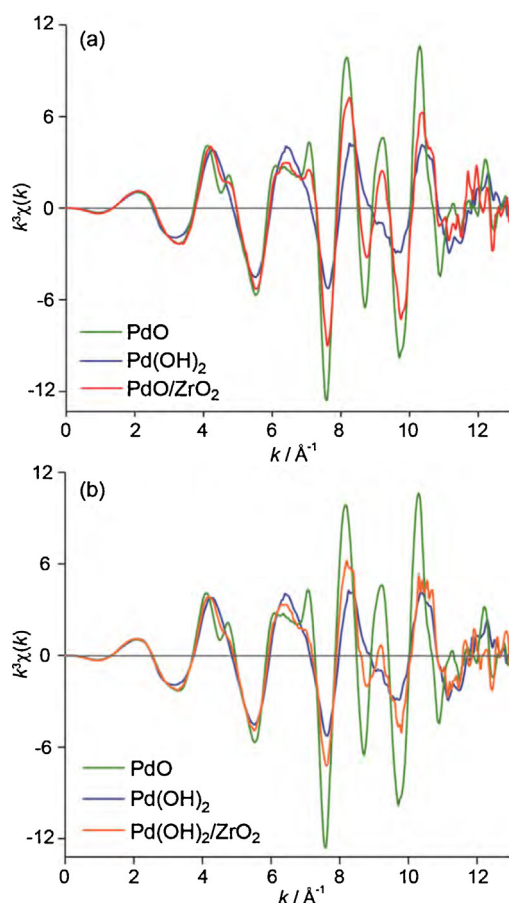
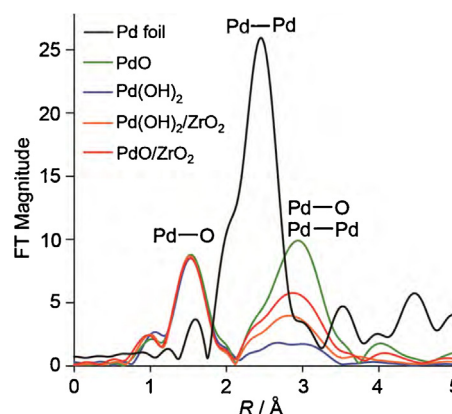
**Fig. 3.** *k*³-weighted Pd K-edge EXAFS oscillations of 10 wt% PdO/ZrO₂ (a) and 10 wt% Pd(OH)₂/ZrO₂ (b) including reference PdO and Pd(OH)₂.**Fig. 4.** Radial structure functions of PdO, 10 wt% PdO/ZrO₂, Pd(OH)₂, and 10 wt% Pd(OH)₂/ZrO₂ (*k* = 2–12 Å^{−1}).

Table 4
Scope of diarylamines and diaryl ethers for Pd(OH)₂/ZrO₂-catalyzed oxidative coupling^a.

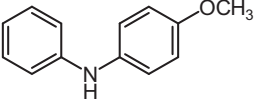
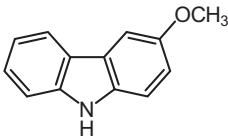
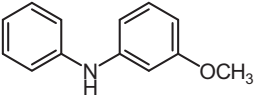
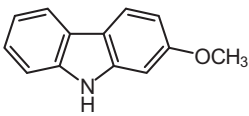
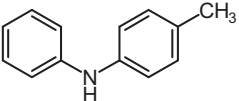
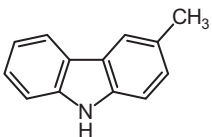
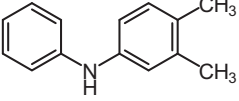
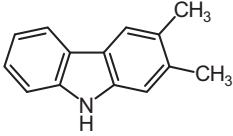
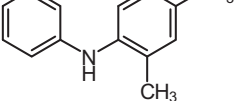
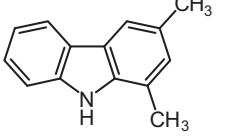
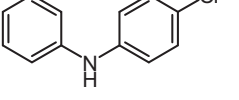
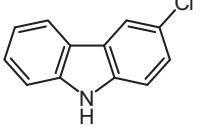
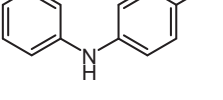
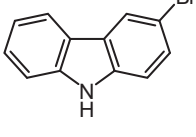
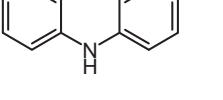
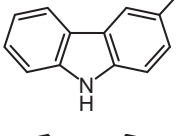
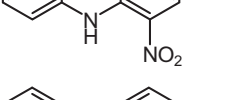
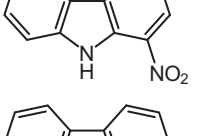
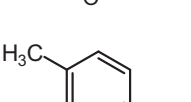
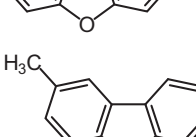
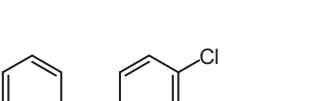
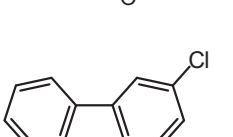


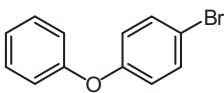
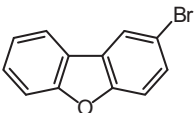
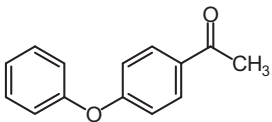
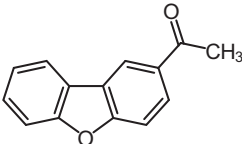
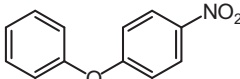
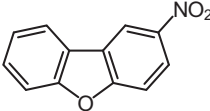
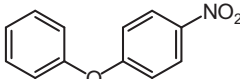
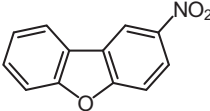
Entry	Substrate	Product	Temp. (°C)	Time (h)	Conv. (%) ^b	Yield (%) ^c
1 ^d			90	6	72	50 (44)
2			90	6	86	(85)
3			90	6	70	67 (60)
4			90	12	91	86 (77)
5			90	6	84	(82)
6			90	12	98	(8)
7			100	18	53	(50)
8			100	18	10	(8)
9 ^e			100	18	64	53 (48)
10			100	18	31	(20)
11 ^f			130	48	88	75 (59)
12 ^f			135	48	97	71 (60)
13 ^f			130	48	89	63 (44)
14 ^f			140	64	86	73

Table 4 (Continued)

Entry	Substrate	Product	Temp. (°C)	Time (h)	Conv. (%) ^b	Yield (%) ^c
15 ^g			130	48	33	9
16 ^f			130	48	96	84 (71)
17 ^f			130	48	60	58
18 ^f			140	64	91	74 (52)

^a Reaction conditions: substrate (1 mmol), 10 wt% Pd(OH)₂/ZrO₂ (50 mg), AcOH (1.5 mL), 1,4-dioxane (1.5 mL), O₂ (0.25 MPa).

^b Calculated on the basis of GC analysis using tridecane as an internal standard.

^c GC yield. Yields in parentheses are isolated yields.

^d Substrate (0.5 mmol).

^e Pd 10 mol%.

^f Substrate (1 mmol), 20 wt% Pd(OH)₂/ZrO₂ (30 mg), PivOH (0.7 g), O₂ (0.5 MPa).

^g Condition f but 20 wt% Pd(OH)₂/ZrO₂ (50 mg).

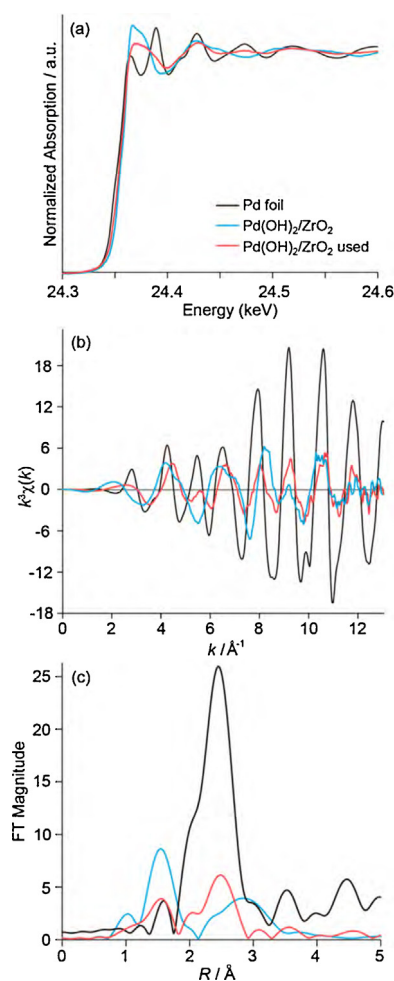


Fig. 5. XAFS results of 10 wt% Pd(OH)₂/ZrO₂ after the synthesis of carbazole including fresh 10 wt% Pd(OH)₂/ZrO₂ and Pd foil for comparison; XANES spectra (a), k^3 -weighted EXAFS oscillations (b), and radial structure functions (c).

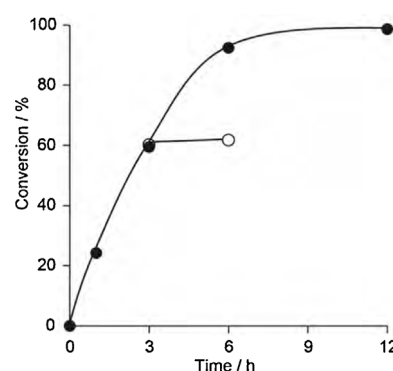


Fig. 6. Intramolecular oxidative coupling of diphenylamine in the presence of Pd(OH)₂/ZrO₂ (●) and after the removal of Pd(OH)₂/ZrO₂ at 3 h by filtration (○). Reaction conditions: diphenylamine (1 mmol), 10 wt% Pd(OH)₂/ZrO₂ (50 mg, Pd 5 mol%), AcOH (1.5 mL), 1,4-dioxane (1.5 mL), O₂ (0.25 MPa), 100 °C.

3.5. Recyclability of catalysts

Recyclability of Pd(OH)₂/ZrO₂ catalysts was examined (Table 5). Although catalytic activities of Pd(OH)₂/ZrO₂ decreased with consecutive runs, the catalyst could be recycled at least three times. Decrease in catalytic activity was probably ascribed to (i) aggregation of Pd species, (ii) leaching of Pd, and (iii) formation of less reactive Pd(0). Increase in the size of Pd NPs after the reaction was only slightly (Fig. 1), thus (i) can be excluded. Although the reaction

Table 5
Recyclability of Pd(OH)₂/ZrO₂ for the synthesis of carbazole^a.

Run	Conv. (%) ^b	Yield (%) ^b	Pd (wt%) ^c
0	–	–	8.2
1	98	85	7.3
2	80	69	6.7
3	74	65	6.2

^a Reaction conditions: diphenylamine (1 mmol), 10 wt% Pd(OH)₂/ZrO₂ (Pd 5 mol%), AcOH (1.5 mL), 1,4-dioxane (1.5 mL), O₂ (0.25 MPa), 100 °C, 12 h.

^b Calculated on the basis of GC analysis.

^c Pd content of the catalysts was analyzed by MP-AES analysis.

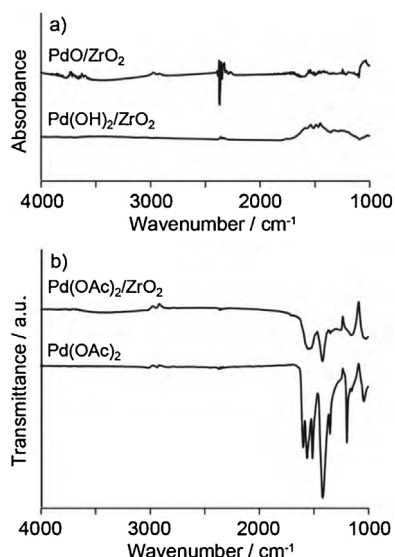
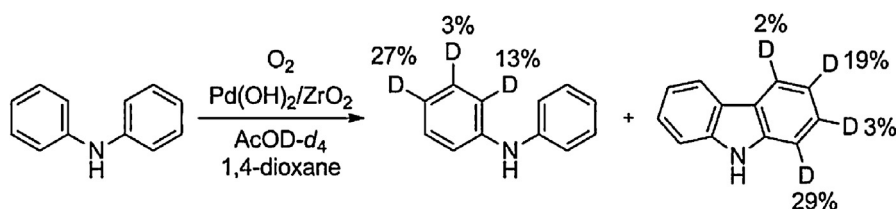


Fig. 7. Difference FT-IR spectra of PdO/ZrO₂ and Pd(OH)₂/ZrO₂ after the oxidative coupling of diphenylamine (a). FT-IR spectra of 10 wt% Pd(OAc)₂/ZrO₂ and Pd(OAc)₂ (b). Reaction conditions: diphenylamine (1 mmol), 10 wt% Pd(OH)₂/ZrO₂ (50 mg), AcOH (1.5 mL), 1,4-dioxane (1.5 mL), O₂ (0.25 MPa), 100 °C, 12 h. After the reaction, the catalysts were washed with CH₂Cl₂, acetone, and H₂O, dried in air at 100 °C for 24 h, and then measured.

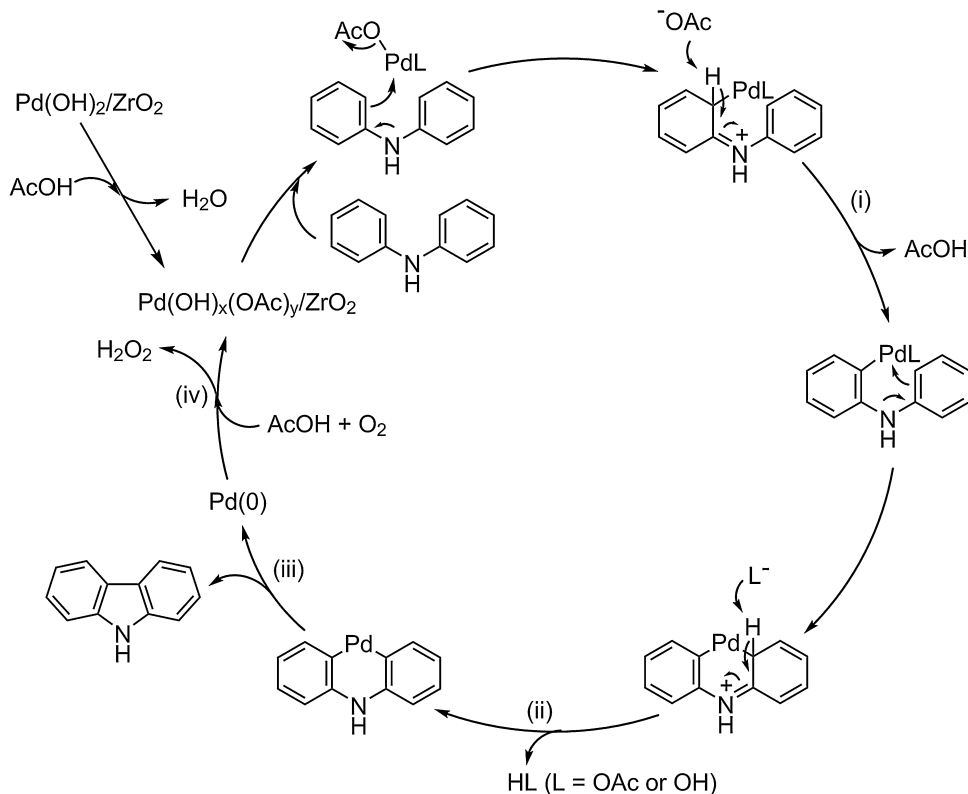
of the filtrate stopped after the removal of the catalyst by filtration at 61% conversion (Fig. 6), (ii) cannot be fully ruled out. Thus, (ii) and (iii) are plausible for catalyst deactivation.

3.6. Possible reaction pathway

To examine whether OH groups of Pd(OH)₂/ZrO₂ are exchanged with acetate during the reaction, FT-IR spectra were obtained. Fig. 7a shows difference spectra of Pd(OH)₂/ZrO₂ between before and after the synthesis of carbazole in AcOH. No peak was observed for PdO/ZrO₂, suggesting that acetate was not adsorbed on the catalyst surface. In contrast, a broad peak was observed for Pd(OH)₂/ZrO₂ from 1360 to 1600 cm⁻¹. These peaks corresponded to COO⁻ stretching (1550–1600 cm⁻¹) and CH₃ deformation (1340–1465 cm⁻¹) vibrations [42], as observed in Pd(OAc)₂/ZrO₂ and reference Pd(OAc)₂ (Fig. 7b). This result revealed that the OH ligands of Pd(OH)₂ on ZrO₂ were partly exchanged with acetate to form catalytically active species during the reaction. In contrast, ligand exchange with acetate hardly occurs for PdO. This was in a good agreement with the observation that PdO showed inferior catalytic activity to Pd(OH)₂. The inferior catalytic activity of Pd(OAc)₂/ZrO₂ compared to that of Pd(OH)₂/ZrO₂ may imply that complete ligand exchange of hydroxy groups with acetate is not essential to promote the reactions.



Scheme 2. Intramolecular coupling of diphenylamine in CD₃CO₂D. Reaction conditions: diphenylamine (1 mmol), 10 wt% Pd(OH)₂/ZrO₂ (50 mg), CD₃CO₂D (1.5 mL), 1,4-dioxane (1.5 mL), O₂ (0.25 MPa), 100 °C, 2 h. H/D exchange ratio was measured by ¹H NMR.



Scheme 3. Possible reaction pathway for the oxidative intramolecular coupling of diphenylamine.

In order to elucidate reaction pathways for the Pd(OH)₂-catalyzed oxidative coupling of diphenylamine, the reaction was performed in CD₃CO₂D (Scheme 2). Unreacted diphenylamine was deuterated at the *o*-, *m*-, and the *p*-positions in 13, 3, and 27%, respectively. The deuterated ratio was in accordance with the reactivity in the electrophilic aromatic substitution reactions. Therefore, the reaction pathway may involve (i) the electrophilic substitution by Pd(II) species to form palladated species [17], (ii) the second substitution to form a palladacycle, (iii) reductive elimination to form carbazole and Pd(0), and (iv) the re-oxidation of Pd(0) to Pd(II) species by O₂ (Scheme 3), although a concerted metalation–deprotonation mechanism [35,43,44] cannot be ruled out. The H/D exchange of the unreacted diphenylamine also ruled out that the step (i) was the rate-determining step.

4. Conclusions

ZrO₂ supported Pd(OH)₂ catalysts promoted the intramolecular oxidative coupling of two C–H bonds of diarylamines and diarylethers to afford the corresponding carbazoles and dibenzofurans with high selectivity using molecular O₂ as a sole oxidant. Supported Pd(OH)₂ exhibited higher catalytic activity than supported PdO and Pd catalysts.

Acknowledgements

This work was financially supported by JST-ALCA (FS Stage). The synchrotron radiation experiments were performed at the BL14B2 in SPring-8 with the approval of JASRI (2011B1001, 2012A1454, and 2012B1075).

Appendix A. Supplementary data

Supplementary data associated with this article can be found, in the online version, at <http://dx.doi.org/10.1016/j.apcatb.2013.12.051>.

References

- [1] L. Yin, J. Liebscher, *Chem. Rev.* 107 (2007) 133–173.
- [2] A.N. Campbell, S.S. Stahl, *Acc. Chem. Res.* 45 (2012) 851–863.
- [3] H.-J. Knölker, K.R. Reddy, *Chem. Rev.* 102 (2002) 4303–4427.
- [4] Y. Zhang, T. Wada, H. Sasabe, *J. Mater. Chem.* 8 (1998) 809–828.
- [5] J. Li, A.C. Grimsdale, *Chem. Soc. Rev.* 39 (2010) 2399–2410.
- [6] D. García-Cuadrado, A.A.C. Braga, F. Maseras, A.M. Echavarren, *J. Am. Chem. Soc.* 128 (2006) 1066–1067.
- [7] M.E. Budén, V.A. Vaillard, S.E. Martin, R.A. Rossi, *J. Org. Chem.* 74 (2009) 4490–4498.
- [8] L.-C. Campeau, M. Parisien, A. Jean, K. Fagnou, *J. Am. Chem. Soc.* 128 (2006) 581–590.
- [9] Z. Liu, R.C. Larock, *Tetrahedron* 63 (2007) 347–355.
- [10] L. Ackermann, A. Althammer, *Angew. Chem. Int. Ed.* 46 (2007) 1627–1629.
- [11] J.L. Wood, B.M. Stoltz, H.-J. Dietrich, D.A. Pflum, D.T. Petsch, *J. Am. Chem. Soc.* 119 (1997) 9641–9651.
- [12] J.A. Jordan-Hore, C.C.C. Johansson, M. Gulias, E.M. Beck, M.J. Gaunt, *J. Am. Chem. Soc.* 130 (2008) 16184–16186.
- [13] S.W. Youn, J.H. Bihn, B.S. Kim, *Org. Lett.* 13 (2011) 3738–3741.
- [14] S. Matsubara, K. Asano, Y. Kajita, M. Yamamoto, *Synthesis* (2007) 2055–2059.
- [15] B. Liégault, D. Lee, M.P. Huestis, D.R. Stuart, K. Fagnou, *J. Org. Chem.* 73 (2008) 5022–5028.
- [16] T. Watanabe, S. Oishi, N. Fujii, H. Ohno, *J. Org. Chem.* 74 (2009) 4720–4726.
- [17] V. Sridharan, M.A. Martín, J.C. Menéndez, *Synlett* (2006) 2375–2378.
- [18] S. Wang, H. Mao, Z. Ni, Y. Pan, *Tetrahedron Lett.* 53 (2012) 505–508.
- [19] T. Watanabe, S. Ueda, S. Inuki, S. Oishi, N. Fujii, H. Ohno, *Chem. Commun.* (2007) 4516–4518.
- [20] V. Sridharan, M.A. Martín, J.C. Menéndez, *Eur. J. Org. Chem.* (2009) 4614–4621.
- [21] S. Hernández, I. Moreno, R.S. Martín, G. Gómez, M.T. Herrero, E. Domínguez, *J. Org. Chem.* 75 (2010) 434–441.
- [22] M. Parisien, D. Valette, K. Fagnou, *J. Org. Chem.* 70 (2005) 7578–7584.
- [23] D. Saha, L. Adak, B.C. Ranu, *Tetrahedron Lett.* 51 (2010) 5624–5627.
- [24] L.L. Chng, J. Zhang, J. Yang, M. Amoura, J.Y. Ying, *Adv. Synth. Catal.* 353 (2011) 2988–2998.
- [25] L.M. Neal, H.E. Hagelin-Weaver, *J. Mol. Catal. A: Chem.* 284 (2008) 141–148.
- [26] C.-T. Yang, Y. Fu, Y.-B. Huang, J. Yi, Q.-X. Guo, L. Liu, *Angew. Chem. Int. Ed.* 48 (2009) 7398–7401.
- [27] S.S. Soomro, F.L. Ansari, K. Chatziapostolou, K. Köhler, *J. Catal.* 273 (2010) 138–146.
- [28] T. Honma, H. Oji, S. Hirayama, Y. Taniguchi, H. Ofuchi, M. Takagaki, *AIP Conf. Proc.* 1234 (2010) 13–16.
- [29] H. Oji, Y. Taniguchi, S. Hirayama, H. Ofuchi, M. Takagaki, T. Honma, *J. Synchrotron Rad.* 19 (2012) 54–59.
- [30] B. Ravel, M. Newville, *J. Synchrotron Rad.* 12 (2005) 537–541.
- [31] G. Brasche, J.G. Fortanet, S.L. Buchwald, *Org. Lett.* 10 (2008) 2207–2210.
- [32] L. Zhou, W. Lu, *Organometallics* 31 (2012) 2124–2127.
- [33] R. Li, L. Jiang, W. Lu, *Organometallics* 25 (2006) 5973–5975.
- [34] M.D.K. Boele, G.P.F. van Strijdonck, A.H.M. de Vries, P.C.J. Kamer, J.G. de Vries, P.W.N.M. van Leeuwen, *J. Am. Chem. Soc.* 124 (2002) 1586–1587.
- [35] M. Lafrance, K. Fagnou, *J. Am. Chem. Soc.* 128 (2006) 16496–16497.
- [36] D.R. Stuart, K. Fagnou, *Science* 316 (2007) 1172–1175.
- [37] Y. Yazawa, H. Yoshida, N. Takagi, S.-i. Komai, A. Satsuma, T. Hattori, *J. Catal.* 187 (1999) 15–23.
- [38] H. Yoshida, T. Nakajima, Y. Yazawa, T. Hattori, *Appl. Catal. B: Environ.* 71 (2007) 70–79.
- [39] R. Yoshimoto, T. Ninomiya, K. Okumura, M. Niwa, *Appl. Catal. B: Environ.* 75 (2007) 175–181.
- [40] X. Guo, M. Meng, F. Dai, Q. Li, Z. Zhang, Z. Jiang, S. Zhang, Y. Huang, *Appl. Catal. B: Environ.* 142–143 (2013) 278–289.
- [41] M. Ren, Y. Kang, W. He, Z. Zou, X. Xue, D.L. Akins, H. Yang, S. Feng, *Appl. Catal. B: Environ.* 104 (2011) 49–53.
- [42] G. Socrates, *Infrared and Raman Characteristic Group Frequencies*, third ed., John Wiley & Sons, Chichester, 2001.
- [43] D. Lapointe, K. Fagnou, *Chem. Lett.* 39 (2010) 1118–1126.
- [44] M. Lafrance, C.N. Rowley, T.K. Woo, K. Fagnou, *J. Am. Chem. Soc.* 128 (2006) 8754–8756.